



Published in final edited form as:

Science. 2007 July 6; 317(5834): 127–130.

## Yeast DNA Polymerase $\epsilon$ Participates in Leading-Strand DNA Replication

Zachary F. Pursell<sup>1</sup>, Isabelle Isoz<sup>2</sup>, Else-Britt Lundström<sup>2</sup>, Erik Johansson<sup>2</sup>, and Thomas A. Kunkel<sup>1\*</sup>

<sup>1</sup>Laboratory of Molecular Genetics and Laboratory of Structural Biology, National Institute of Environmental Health Sciences, NIH, DHHS, Research Triangle Park, NC 27709, USA.

<sup>2</sup>Department of Medical Biochemistry and Biophysics, Umeå University, SE-901 87, Umeå, Sweden.

### Abstract

Multiple DNA polymerases participate in replicating the leading and lagging strands of the eukaryotic nuclear genome. Although 50 years have passed since the first DNA polymerase was discovered, the identity of the major polymerase used for leading-strand replication is uncertain. We constructed a derivative of yeast DNA polymerase  $\epsilon$  that retains high replication activity but has strongly reduced replication fidelity, particularly for thymine-deoxythymidine 5'-monophosphate (T-dTMP) but not adenine-deoxyadenosine 5'-monophosphate (A-dAMP) mismatches. Yeast strains with this DNA polymerase  $\epsilon$  allele have elevated rates of T to A substitution mutations. The position and rate of these substitutions depend on the orientation of the mutational reporter and its location relative to origins of DNA replication and reveal a pattern indicating that DNA polymerase  $\epsilon$  participates in leading-strand DNA replication.

Replication of the eukaryotic nuclear genome requires DNA polymerase  $\alpha$  to initiate synthesis at origins and to initiate synthesis of Okazaki fragments on the lagging strand, allowing DNA polymerases  $\delta$  (pol  $\delta$ ) and  $\epsilon$  (pol  $\epsilon$ ) to then perform the bulk of chain elongation (1,2). Pol  $\delta$  is implicated in lagging-strand replication (1), but the identity of the polymerase(s) that replicates the leading strand is unknown (1,2). Null alleles of the *POL2* (pol  $\epsilon$ ) and *POL3* (pol  $\delta$ ) genes are uninformative for identifying the leading-strand polymerase, because both genes are essential for normal replication. To retain replication activity while generating a distinct mutational signature in vivo that allows assignment of pol  $\epsilon$  to leading- and/or lagging-strand replication in yeast cells, we substituted glycine for Met<sup>644</sup> at the *Saccharomyces cerevisiae* pol  $\epsilon$  active site. Yeast pol  $\epsilon$  with the Met<sup>644</sup>Gly change retains 44% of wild-type polymerase activity (Fig. 1A) and retains full 3' exonuclease activity (Fig. 1B). A haploid *pol2-M644G* yeast strain grows at a rate similar to a *POL2* strain (Fig. 1C), indicating that M<sup>644</sup>G pol  $\epsilon$  retains substantial replicative capacity. In both its exonuclease-proficient (Fig. 1D) and exonuclease-deficient forms (Fig. 1E), M<sup>644</sup>G pol  $\epsilon$  synthesizes DNA in vitro with reduced fidelity in comparison with wild-type (i.e., Met<sup>644</sup>) pol  $\epsilon$  (Fig. 1 and table S1) (3), i.e., it is defective in discriminating against deoxynucleotide triphosphate (dNTP) misinsertion. Even the exonuclease-proficient polymerase has an elevated base-substitution error rate (Fig. 1D), indicating that despite retaining proofreading potential (Fig. 1B), M<sup>644</sup>G pol  $\epsilon$  does not efficiently proofread certain mismatches, for example, T-dTMP mismatches. This is more obvious in some sequence contexts than others. Among 16 positions in the *lacZ* template where T to A substitutions can be detected (fig. S1), errors are particularly prevalent at template T

\*To whom correspondence should be addressed. E-mail: kunkel@niehs.nih.gov.

+147 and T-36 (Fig. 1F), resulting in a high error rate of exonuclease-proficient M<sup>644</sup>G pol ε for T-dTMP mismatches ( $11 \times 10^{-5}$ ). In contrast, the lowest error rate for exonuclease-proficient M<sup>644</sup>G pol ε is  $\leq 0.28 \times 10^{-5}$  for the A-dAMP mismatch, a difference of at least 39-fold (Fig. 1D). This large difference in the rate of stable misincorporation of dTMP opposite T compared to dAMP opposite A is critical for interpreting M<sup>644</sup>G pol ε's distinctive mutational signature in yeast, because these mismatches are the two possible intermediates that could result in an A-T to T-A substitution in vivo.

In haploid yeast containing the exonuclease-proficient *pol2-M644G* allele, the spontaneous mutation rate at the *CAN1* locus was elevated by a factor of 3.9 compared with a wild-type strain (table S3) (3). When repair of single-base mismatches was inactivated by disrupting *MSH6*, the mutation rate at *CAN1* in the *pol2-M644G* strain was 58 times as high as that for the *Δmsh6* strain with wild-type *POL2* (table S3), consistent with inaccurate DNA replication in vivo by exonuclease-proficient M<sup>644</sup>G pol ε. When 11 independent *Can<sup>r</sup>* mutants from the *pol2-M644G* strain were sequenced, six contained T-A to A-T substitutions predicted by the high rate of T-dTMP mismatch formation by M<sup>644</sup>G pol ε (Fig. 1D).

Based on these results, we investigated whether M<sup>644</sup>G pol ε participates in leading-and/or lagging-strand replication using a strategy previously employed to follow replicative mutagenesis on the two strands in strains encoding wild-type or exonuclease-deficient DNA polymerases (4–6). In those studies, the template strand for replication errors was assigned by monitoring incorporation of 6-hydroxylaminopurine monophosphate opposite template cytosine on one strand, or incorporation of dAMP opposite template 8-oxo-G on the other strand. In the present study, we assigned the template strand based on the strong preference of M<sup>644</sup>G pol ε for stable misincorporation of dTMP opposite T rather than dAMP opposite template A (Fig. 1D). We compared spontaneous mutation rates in strains containing the *pol2-M644G* allele or the wild-type *POL2* gene (Table 1). Rates were measured using the *URA3* reporter gene, which was inserted in each of the two possible orientations, and on opposite sides of, but close to, ARS306 (Fig. 2), an origin of replication on the left arm of chromosome III that fires in early S phase with >90% efficiency (7).

*URA3* mutation rates in the wild-type *POL2* strains ranged from  $3.1 \times 10^{-8}$  to  $6.6 \times 10^{-8}$ , whereas rates in the *pol2-M644G* strains ranged from  $16 \times 10^{-8}$  to  $45 \times 10^{-8}$  (Table 1). When independent *ura3* mutants from these strains were sequenced, a variety of mutations were observed in the wild-type (M644) strains, consistent with many sources of mutagenesis in wild-type yeast. Among the mutations, A-T to T-A substitutions were rare, resulting in low spontaneous mutation rates for these two events in wild-type strains (Table 1). In contrast, and as predicted by the high rate of T-dTMP mismatch formation by M<sup>644</sup>G pol ε in vitro (Fig. 1D), the rates of A-T to T-A substitutions were higher in the *pol2-M644G* strains (Table 1). Just as misincorporation in vitro was prevalent at certain template locations in the *lacZ* template (e.g., T+147 and T-36, Fig. 1F), the majority of these transversions generated in the *pol2-M644G* strains occurred at two specific base pairs (hot spots) in the *URA3* coding sequence, numbers 279 and 686 (Fig. 2).

The rate of these substitutions depended strongly on the orientation and location of the *URA3* gene. When *URA3* was placed to the right of ARS306 in the *pol2-M644G* strain, 43 of 61 mutants recovered contained an A to T transversion, defined relative to the *URA3* coding strand (Table 1), and 36 of these 43 were at base pair number 686 (Fig. 2A). This yields a rate of A to T transversion at base pair 686 in orientation 1 of  $13 \times 10^{-8}$  (Fig. 2A). This rate is higher than that observed in the corresponding wild-type strain ( $\leq 0.6 \times 10^{-8}$ ) (Fig. 2A), which indicates that the A to T mutations are dependent on replication by M<sup>644</sup>G pol ε. Because ARS306 is only ~1700 base pairs distant from the *URA3* gene, the replication fork emanating from ARS306 reaches base pair 686 long before the fork emanating from ARS307, which is

over 32,000 base pairs to the right of *URA3*. In this case, if we assume from the error specificity in vitro (Fig. 1D) that these events resulted from T-dTMP mismatches generated by M<sup>644</sup>G pol  $\epsilon$  rather than by A-dAMP mismatches, pol  $\epsilon$  is inferred to replicate the leading-strand template, as depicted in Fig. 2A.

In contrast to the two A to T hot spots, only two T to A events were detected among 61 mutations recovered from this strain (Table 1, R-ARS306, orientation 1), even though there are many sites where such substitutions can be scored. Such T to A events would be inferred to result from T-dTMP mismatches generated if M<sup>644</sup>G pol  $\epsilon$  was replicating the lagging-strand DNA template. This paucity of T to A substitutions could be due to the fact that pol  $\epsilon$  participates much more in leading-strand replication than in lagging-strand replication. Alternatively, a hot spot sequence context may not be present in the lagging-strand template. These two possibilities were distinguished by comparing results in a second strain in which *URA3* was again placed to the right of ARS306, but now in the opposite orientation. In orientation 2, where a T-dTMP mismatch at base pair 686 would be a lagging-strand error, the rate of A to T transversions at base pair 686 was observed to be lower by a factor of at least 32 ( $\leq 0.4 \times 10^{-8}$ , Fig. 2B) as that in orientation 1. Thus, the lack of T to A substitutions in orientation 1 is not simply due to the absence of the appropriate hot spot sequence context in the lagging-strand template, but is most simply explained by prominent participation of pol  $\epsilon$  in leading-strand replication as compared with lagging-strand replication.

This interpretation is reinforced by the fact that the opposite mutational asymmetry holds when *URA3* is located to the left of ARS306. Here, the rate of A to T transversions at base pair 686 was high ( $20 \times 10^{-8}$ ) in orientation 2 (Fig. 2C), where a T-dTMP mismatch by M<sup>644</sup>G pol  $\epsilon$  would again be a leading-strand error, and the rate is lower by at least a factor of 25 ( $\leq 0.5 \times 10^{-8}$ ) in orientation 1 (Fig. 2D), where a T-dTMP mismatch would be a lagging-strand error. These effects are not confined to the A–T base pair at position 686, because a similar pattern is observed at position 279 in the *URA3* gene (Fig. 2). A to T substitutions at position 279 are only seen in two of the four strains (Fig. 2, A and C), and in both cases the pattern is consistent with T-dTMP mismatches generated by M<sup>644</sup>G pol  $\epsilon$  during replication of the leading-strand template. Finally, a similar pattern is observed at a second genomic location examined by inserting *URA3* in opposite orientations 850 base pairs to the right of ARS501, an origin of replication on the right arm of chromosome V that is used late in S phase (8). The results at ARS501 are similar to those at ARS306, in that the rate of A to T transversion at base pair 686 is 11 times as high in orientation 1 (Table 1 and Fig. 2E) compared with orientation 2 (Table 1 and Fig. 2F). Given that the nearest flanking origin is at least 10,000 base pairs to the right of ARS501, this pattern is consistent with T-dTMP mismatches generated by M<sup>644</sup>G pol  $\epsilon$  during replication of the leading-strand template.

From the M<sup>644</sup>G pol  $\epsilon$  bias for T-dTMP as opposed to A-dAMP errors (Fig. 1) and the patterns of mutagenesis in vivo (Fig. 2), we infer that M<sup>644</sup>G pol  $\epsilon$ , and therefore likely wild-type pol  $\epsilon$ , participates in leading-strand replication. This interpretation is consistent with evidence for pol  $\delta$  participation in lagging-strand replication (1) and with evidence that the exonuclease activities of pol  $\delta$  and pol  $\epsilon$  edit 6-hydroxylaminopurine-induced mismatches on opposite strands (6). The interpretation that pol  $\epsilon$  replicates the leading strand does not exclude its participation in lagging-strand replication under certain circumstances. The interpretation also does not exclude the possibility that pol  $\delta$  might contribute to leading-strand replication. Both models for the participation of pol  $\delta$  and pol  $\epsilon$  in leading- and lagging-strand replication (1,2) may be correct, with the choice of polymerase dependent on such variables as replication timing (9), DNA sequence context, chromosomal organization and/or chromatin status, or various types of replicative stress. Given that pol  $\epsilon$  is a known checkpoint sensor (10–12), our evidence that pol  $\epsilon$  has an important role in replicating the leading strand is consistent with the idea that

the status of leading-strand synthesis of replication fork progression determines whether the S phase checkpoint is activated (13,14).

## References and Notes

1. Garg P, Burgers PM. *Crit. Rev. Biochem. Mol. Biol* 2005;40:115. [PubMed: 15814431]
2. Johnson A, O'Donnell M. *Annu. Rev. Biochem* 2005;74:283. [PubMed: 15952889]
3. Materials and methods are available as supporting material on *Science Online*.
4. Pavlov YI, Mian IM, Kunkel TA. *Curr. Biol* 2003;13:744. [PubMed: 12725731]
5. Pavlov YI, Newlon CS, Kunkel TA. *Mol. Cell* 2002;10:207. [PubMed: 12150920]
6. Shcherbakova PV, Pavlov YI. *Genetics* 1996;142:717. [PubMed: 8849882]
7. Poloumienko A, Dershowitz A, De J, Newlon CS. *Mol. Biol. Cell* 2001;12:3317. [PubMed: 11694569]
8. Ferguson BM, Brewer BJ, Reynolds AE, Fangman WL. *Cell* 1991;65:507. [PubMed: 2018976]
9. Fuss J, Linn S. *J. Biol. Chem* 2002;277:8658. [PubMed: 11741962]
10. Dua R, Edwards S, Levy DL, Campbell JL. *J. Biol. Chem* 2000;275:28816. [PubMed: 10878005]
11. Dua R, Levy DL, Campbell JL. *J. Biol. Chem* 1999;274:22283. [PubMed: 10428796]
12. Navas TA, Zhou Z, Elledge SJ. *Cell* 1995;80:29. [PubMed: 7813016]
13. Harrison JC, Haber JE. *Annu. Rev. Genet* 2006;40:209. [PubMed: 16805667]
14. Sancar A, Lindsey-Boltz LA, Unsal-Kacmaz K, Linn S. *Annu. Rev. Biochem* 2004;73:39. [PubMed: 15189136]
15. Shcherbakova PV, Kunkel TA. *Mol. Cell. Biol* 1999;19:3177. [PubMed: 10082584]
16. We thank D. Nguyen for DNA substrate preparation and sequence analysis of lacZ mutants, and R. Schaaper and D. Gordenin for critically reading this manuscript. This work was funded in part by the Intramural Research Program of the NIH, National Institute of Environmental Health Sciences (T.A.K.) and partly by the Swedish Research Council, The Swedish Cancer Society, and the Fund for Basic Science-Oriented Biotechnology and the Medical Faculty at Umeå University (E.J.).

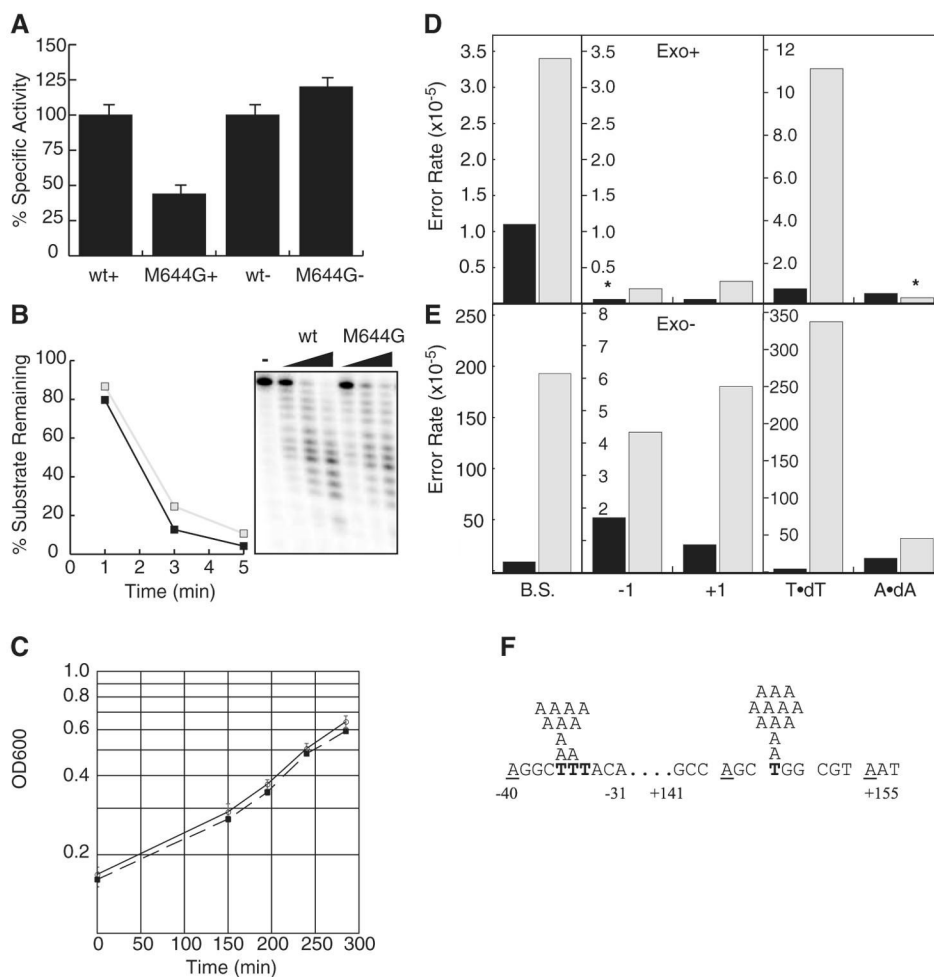


**Fig. 1.** Specific activity, growth, and fidelity analyses of  $M^{644}G$  pol  $\epsilon$ . **(A)** Relative specific activity of pol  $\epsilon$  derivatives with activated DNA. **(B)** Exonuclease activity of wild-type (black boxes) and  $M^{644}G$  pol  $\epsilon$  (gray boxes). **(C)** Growth curves for wild-type (solid line) and *pol2-M644G* (dashed line) strains. **(D)** Average error rates for exonuclease-proficient wild-type (black bars) and  $M^{644}G$  pol  $\epsilon$  (gray bars) for base substitutions (B.S.), single-base deletions (-1), single-base insertions (+1), T to A transversions (*T•dT*), and A to T transversions (*A•dA*). Asterisks denote error rates that are  $\leq$  the indicated value. **(E)** As in (D) but for exonuclease-deficient pol  $\epsilon$ . **(F)** T to A transversions at -36 and +147 positions in *lacZ* using exonuclease-proficient  $M^{644}G$  pol  $\epsilon$ . Sites where T to A and A to T transversions are detectable are in bold and underlined, respectively.

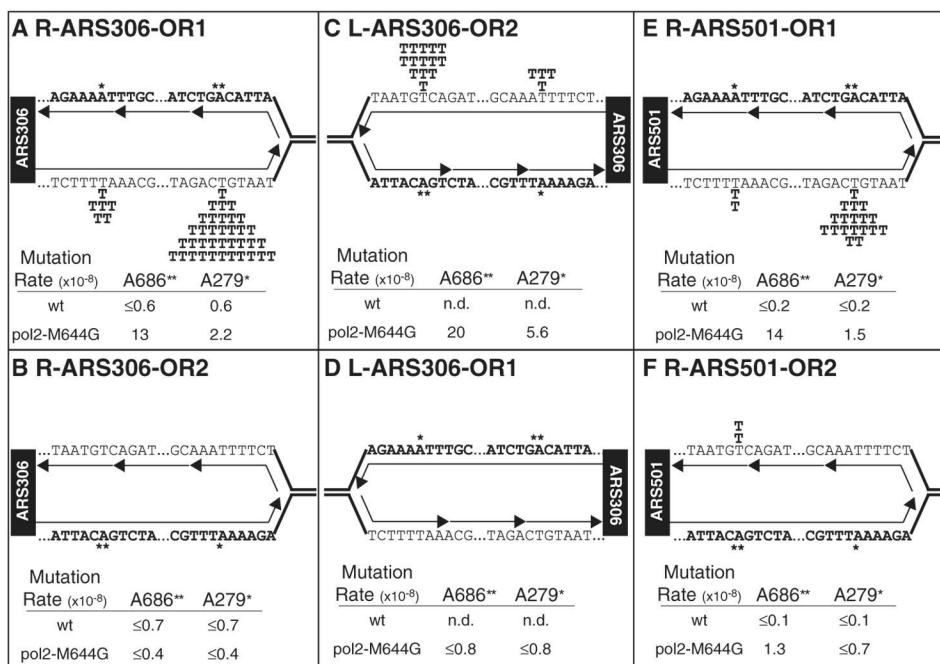


**Fig. 2.** Variation in the rates of T to A transversions by location and gene orientation. Six haploid strains were constructed containing the *pol2-M644G* mutant allele. *URA3* was to the right (**A**, **B**, **E**, and **F**) or left (**C** and **D**) of the indicated ARS, with the coding sequence in the Watson (A, D, and E) or Crick (B, C, and F) strand. A replication fork is shown moving away from the ARS (black box) and replicating the *URA3* gene. The nascent leading strand is depicted as a single, unbroken arrow, whereas nascent Okazaki fragments on the lagging strand are depicted as broken arrows. The A–T to T–A hot spots (\* for A279 and \*\* for A686) are represented as the inferred T–dTMP mispair generated during replication.

Table 1

Mutation rates at *URA3*. Mutation rates were measured as described in (15). Parentheses contain the numbers of A-T to T-A plus T-A to A-T substitutions observed among the total number of *ura3* mutants sequenced. CI, confidence interval.

Yeast strain	Location and origin	<i>URA3</i> orient.	Mut. rate ( $\times 10^{-8}$ )	95% CI	A-T to T-A plus T-A to A-T ( $\times 10^{-8}$ )	Occurrences A-T to T-A to A-T
Wild type	R-ARS306	1	6.6	3.5-12	1.6 (3/12)	2:1
		2	5.9	1.6-17	1.5 (2/8)	1:1
pol2-M644G	L-ARS306	1	16	11-36	5.3 (7/21)	1:6
		2	45	23-60	29 (20/31)	18:2
	R-ARS306	1	28	13-40	19 (45/61)	43:2
		2	16	9.7-36	2.1 (5/38)	1:4
Wild type	R-ARS501	1	3.9	3.2-7.2	0.16 (1/24)	0:1
		2	3.1	2.2-6.4	0.25 (2/25)	1:1
pol2-M644G	R-ARS501	1	26	17-40	17 (22/34)	22:0
		2	21	15-44	5.9 (9/32)	2:7